Submillimeter Heterodyne Detection of Interstellar Carbon Monoxide at 434 Micrometers

Abstract. *A submillimeter heterodyne radiometer, developed for astronomical applications, uses an optically pumped laser local oscillator and a quasi-optical Schottky diode mixer. The resultant telescope-mounted system, which has a noise temperature less than 4000 K (double sideband) and high frequency and spatial resolution, has been used to detect the* $J = 6 \rightarrow 5$ *rotational transition of carbon monoxide at 434 micrometers in the Orion molecular cloud. The measurements, when compared with previous millimeter-wave data, indicate that the broad carbon monoxide emission feature is produced by an optically thin gas whose temperature exceeds 180 K.*

Submillimeter astronomy has been relatively slow in developing because of a lack of both sensitive detectors and suitable observing sites. High-resolution spectroscopy at wavelengths (λ) shorter than 500 μm has eluded earthbound astronomers because the opacity of the atmosphere increases beyond about $\lambda = 1$ mm due to water vapor absorption (*1*). However, since many interstellar molecular and several atomic species have important transitions in this region, there is growing interest in these wavelengths. Several excellent new telescopes have been built at altitudes and locations with relatively good atmospheric transmission. We report here laser heterodyne observations in this wavelength region, which were made at the NASA Infrared Telescope Facility (IRTF), situated at an altitude of 4200 m on Mauna Kea, Hawaii. In this experiment, emission from the $J = 6 \rightarrow 5$ rotational transition of CO from the molecular cloud in Orion was detected at 434 μm (691.4726 GHz). The specially designed system that was used is the result of progress in the development of laser heterodyne radiometers and has the potential for detection and mapping of a variety of less abundant molecules.

The presence of CO in the Orion Nebula was observed previously, at 118 μm with incoherent detectors from aircraft (*2*) and at lower frequencies with coherent techniques employing the InSb hot electron bolometer (*3, 4*) and GaAs Schottky diodes (*5*). Earlier observations had indicated that there is a very extended region (angular size greater than 30 arc minutes, corresponding to a linear dimension greater than 1.5×10^{19} cm) with a gas temperature of 20 to 60 K and an emission line width of 4 to 5 km/sec (*6*). However, of special interest is the core region containing the Kleinmann-Low and Becklin-Neugebauer infrared objects. Here a low-level "plateau" emission feature with a line width greater than 100 km/sec and an angular size less than 1 arc minute has been observed (*7, 8*). Analysis of emission spectra of this gas in the $J = 2 \rightarrow 1$ and $J = 3 \rightarrow 2$ rotational transitions of CO suggested that the CO is optically thin and significantly hotter than the surrounding molecular material (*4*). Near-infrared observations of H_2 emission (*9*) have contributed to the current model of this region, which consists of an expanding shock interacting with the ambient molecular cloud (*10*).

The lack of high-frequency data has hampered refinement of the theoretical model for this region, which is important for determining the driving force behind the shock [possibly a supernova event (*8*) or a very young star (*11*)]. In addition, the temperature and density of the shocked gas are critical parameters for assessing the chemistry taking place there, which can drastically alter the abundance of certain species (*12*). Submillimeter observations are important since lines in this wavelength range are particularly sensitive to the temperatures believed to prevail in this shock-heated region. In the experiment reported here we measured the temperature and line width of the higher frequency CO transition and found both to be greater than those of the lower transitions.

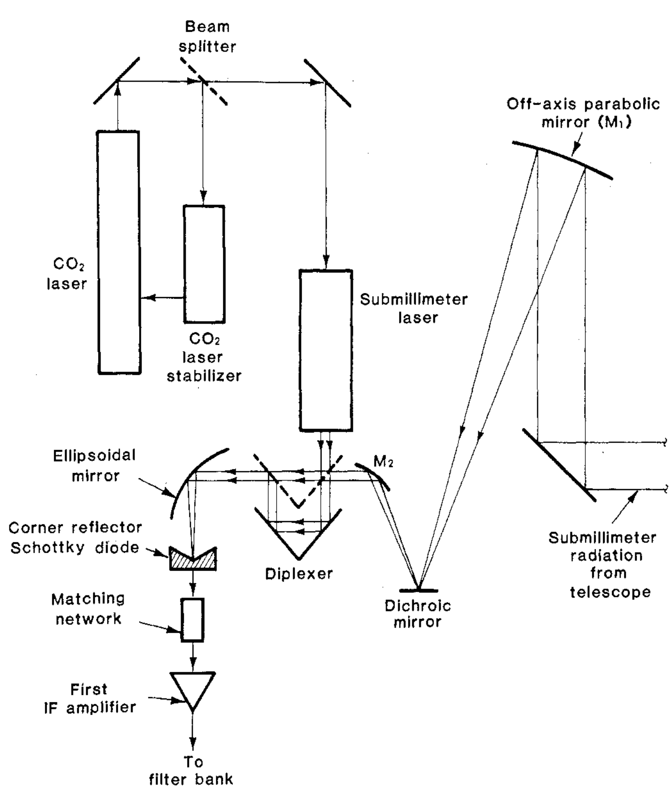

Fig. 1. Experimental setup at the telescope includes a stabilized optically pumped submillimeter laser local oscillator and a quasi-optical system to couple radiation from the telescope to the Schottky diode mixer.

The concept of heterodyne detection, widely used at microwave and millimeter wavelengths, allows extremely high frequency resolution and sensitivity by converting the spectral distribution of energy at the signal frequency to a much lower frequency. At the lower frequency, a filter of a given bandwidth corresponds to a very high fractional resolution. The system we developed incorporates heterodyne detection, but relies on an optically pumped laser local oscillator (LO) and quasi-optical techniques rather than the waveguides and microwave instrumentation used in conventional radio astronomical observations.

The heterodyne mixer element is a very low capacitance GaAs Schottky diode (one of an array of several hundred diodes ~ 1 μm in diameter fabricated on a 0.25-mm-square semiconductor chip), which was chosen over other devices for its superior bandwidth and sensitivity. The diode chip is mounted in a recently developed corner reflector configuration (*13*), and one of the diodes is contacted by a long-wire whisker antenna. The radiation patterns from a number of these corner reflectors were measured, and de-

0036-8075/81/0206-0580$00.50/0

vices having good mode quality as well as low noise temperature were selected for the telescope experiment. An appropriate matching network and field effect transistor (FET) amplifier (*14*) (intermediate frequency, 1.4 GHz; noise temperature, 50 K) were constructed, which resulted in a total double-sideband (DSB) system noise temperature of 3000 K in the laboratory and $\lesssim$ 3900 K at the telescope. This represents an improvement of approximately a factor of 3 in sensitivity over the best results reported previously at these frequencies (*13*).

Since the LO, consisting of a CO_2 laser pumping a far-infrared waveguide laser, was bulky and could not be mounted directly on the telescope, the entire system was placed at the fixed (coudé) focus of the 3-m telescope. The system was then coupled to the telescope, using a set of off-axis parabolic mirrors to reduce the beam diameter by a factor of 5 from that produced by the coudé system, which had a ratio of focal length to lens diameter (*f/D*) of 120. A dichroic mirror, coated with 150 Å of gold, was placed at the focal plane and permitted visual sighting of objects while reflecting more than 95 percent of the submillimeter radiation. The entire system is shown in Fig. 1.

The wavelength and power requirements for this experiment effectively restricted the choice of LO to an optically pumped formic acid laser. The laser LO, which needed a submillimeter output power of 15 to 20 mW to drive the mixer diode, was a severe problem because existing systems typically were not sufficiently stable for the required integration times. Since one of the major sources of instability of such a laser is feedback of the pump laser, an off-axis beam injection approach was chosen, which eventually produced almost complete isolation. An external tunable etalon was used to frequency-lock the 30-W CO_2 pump laser, while the submillimeter cavity was passively stabilized with invar rods and compensating aluminum sleeves (*15*). To transport and use this system at 4200-m altitude, the entire apparatus was reinforced. The electronics and high-voltage supply were tested in a high-altitude chamber and insulation was added where required to permit operation at reduced pressures. The LO output power was measured and found to be constant within 4 percent over periods of hours.

The received signal and the laser LO are combined in an optical diplexer (*13*) and mixed in the GaAs Schottky diode; the difference frequency is then amplified by the low-noise FET amplifier and fed to a filter bank of 32 discrete 1-MHZ and 32 discrete 5-MHz filters for spectral analysis (*16*). A resolution of 5 MHz corresponds to $\lambda/\Delta\lambda = 1.4 \times 10^5$ at the frequency of the $J = 6 \rightarrow 5$ transition of CO. From the filters, the signal was sent to a minicomputer, which controlled the beam switching of the telescope and recorded the data.

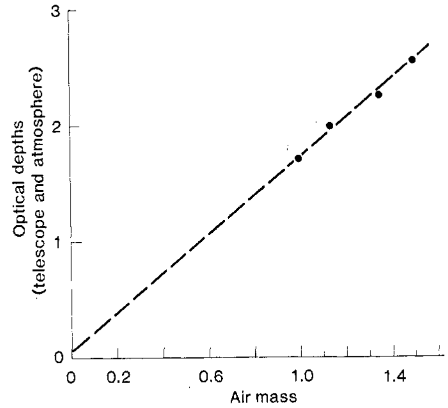

Fig. 2. Total optical depth (τ) as a function of telescope pointing angle z from zenith expressed in terms of air mass A, where A = sec z. Spillover around the subreflector arising from the significant sidelobe content of the corner reflector radiation pattern is not included in τ.

Even from a high, dry site such as Mauna Kea, the atmospheric transmission at 434 μm is highly variable and acceptable for astronomical observations only a small fraction of the time (*17*). The atmospheric transmission was measured by comparing the signal received when the telescope was pointed at the cold sky background with that from a cold absorber at 77 K. The atmospheric transmission coefficient τ was then obtained from T (emission) = T (ambient) $\times$ $(1 - e^{-\tau})$, where T is temperature and τ includes the transmission losses in the optics of the telescope system. This should be a reasonable approximation since the H_2O producing the opacity is confined to elevations not greatly exceeding that of the observatory. Figure 2 shows the optical depth during our best observation period as a function of telescope pointing angle z from zenith; it is expressed in terms of air mass A, where A = sec z. During our observing runs the optical depth varied from 1.7 to 3 per air mass. Theoretical calculations (*17, 18*) indicate that the optical depth at the observing frequency is given by $\tau = 1.3 \times$ (millimeters of precipitable H_2O). Using this relation, we infer that the precipitable water vapor varied between 1.3 and 2.4 mm during our observing run. This range of values is consistent with prevailing site conditions during our observations.

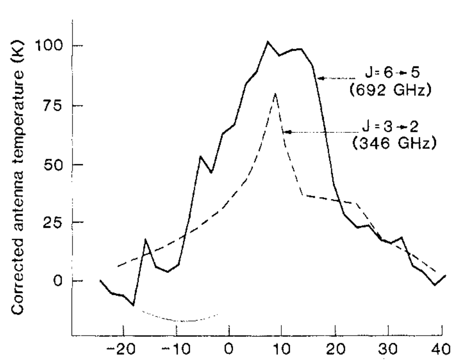

Fig. 3. Measured CO emission from Orion. The $J = 6 \rightarrow 5$ spectrum is from this experiment and the $J = 3 \rightarrow 2$ spectrum is from (*4*). The data were corrected for atmospheric absorption and telescope beam efficiency.

Only the $J = 6 \rightarrow 5$ emission at 434 μm was spectrally analyzed with the filter bank. By means of a beam-switching technique, the difference in signal when the telescope was pointed on and off Orion was averaged over periods of 10 to 15 minutes. The resulting output of the 5-MHz filter bank is displayed in Fig. 3. The peak antenna temperature is 100 K (blackbody temperature to produce equivalent flux), and the full width at half-maximum of the spectral line is approximately 60 MHz, or 26 km/sec when expressed in terms of the equivalent Doppler velocity of the molecular cloud. The spectrum is corrected for atmospheric transmission and for telescope beam efficiency (0.36) determined by observation of Venus (*19*). The root-mean-square noise calculated from the measured system temperature, and scaled in the same manner as the data to account for atmospheric attenuation and beam efficiency, is 6 K. The actual uncertainty in the intensity is dominated by uncertainties in the correction factors and is estimated to be ~ 20 percent. Both the peak temperature and line width are greater than those observed in the lower CO transitions (*4, 7, 8*). (If there is significant emission outside the limits of our filter bank, the $J = 6 \rightarrow 5$ line is even stronger than indicated in Fig. 3.) Comparison of the ratio of the intensity of the $6 \rightarrow 5$ emission from the present experiment to that of the previously measured $3 \rightarrow 2$ emission, using a collisional excitation model for CO (*20*), supports the interpretation that the source of the broad CO emission feature is optically thin (opacity < 1). The different behavior of the narrow line source and broad component source as a function of J is due to the former being optically thick and thermalized (antenna temperature independent of J), while the latter, if hot and optically thin, has an antenna temperature $\propto J^2$. More detailed calculations including the effects of radiative transfer (*21*) show that this gas is in a hot region and has an excitation temperature > 180 K, considerably higher than previous lower limits. Since the values derived from the density of the gas indicate that the transitions up through $J = 6$ are essentially thermalized, the excitation temperature should be close to the gas kinetic temperature. The more detailed analysis (*21*) indicates that the fractional abundance of CO appears to be reduced by a factor of 5 in this region compared to that typical of interstellar clouds.

These initial observations demonstrate that high-resolution ground-based submillimeter astronomy can add significantly to our understanding of active regions in interstellar molecular clouds. The angular resolution achievable at submillimeter wavelengths with modest-sized telescopes is comparable to the highest obtained with any single radio antenna (~ 30 arc seconds). A next step would be to accurately map the spatial distribution and homogeneity of CO in the central regions of interstellar clouds. In addition, with modest improvements in sensitivity, a wide variety of molecular lines should be accessible for study by astronomers.

H. R. FETTERMAN
Lincoln Laboratory, Massachusetts Institute of Technology, Lexington 02173
G. A. KOEPF
Phoenix Corporation, 1700 Old Meadow Road, McLean, Virginia 22120
P. F. GOLDSMITH
Five College Radio Astronomy Observatory, University of Massachusetts, Amherst 01003
B. J. CLIFTON
Lincoln Laboratory, Massachusetts Institute of Technology
D. BUHL
NASA/Goddard Space Flight Center, Greenbelt, Maryland 20771
N. R. ERICKSON
Five College Radio Astronomy Observatory, University of Massachusetts
D. D. PECK
Lincoln Laboratory, Massachusetts Institute of Technology
N. MCAVOY
NASA/Goddard Space Flight Center
P. E. TANNENWALD
Lincoln Laboratory, Massachusetts Institute of Technology

References and Notes

1. Not until the near-infrared windows in the 10-μm region is the atmospheric transmission sufficiently high to permit ground-based heterodyne astronomical observations [A. L. Betz, M. A. Johnson, R. A. McLaren, E. C. Sutton, *Astrophys. J.* **208**, L141 (1976); T. Kostiuk, M. J. Mumma, J. J. Hillman, D. Buhl, L. W. Brown, J. L. Fans, D. L. Spears, *Infrared Phys.* **17**, 431 (1977)]. On the other hand, measurements with incoherent detection have been carried out extensively throughout the far-infrared region, both from the ground and from aircraft [J. Smith, D. K. Lynch, D. Cudaback, M. W. Werner, *Astrophys. J.* **234**, 902 (1979); D. M. Watson *et al.* (*2*)].
2. D. M. Watson, J. W. V. Storey, C. H. Townes, E. E. Haller, W. L. Hansen, *Astrophys. J. Lett.*, in press.
3. P. G. Wannier and T. G. Phillips, *Astrophys. J.* **215**, 796 (1977).
4. T. G. Phillips, P. J. Huggins, G. Neugebauer, M. W. Werner, *ibid.* **217**, L161 (1977).
5. N. R. Erickson, *IEEE International Microwave Symposium Digest, Ottawa* (IEEE, New York, 1978), p. 438.
6. R. A. Linke and P. G. Wannier, *Astrophys. J.* **193**, L41 (1974).
7. B. Zuckerman, T. B. H. Kuiper, E. N. Rodriguez-Kuiper, *ibid.* **209**, L137 (1976).
8. J. Kwan and N. Z. Scoville, *ibid.* **210**, L39 (1976).
9. T. N. Gautier, U. Fink, R. R. Treffers, H. P. Larson, *ibid.* **207**, L129 (1976).
10. J. Kwan, *ibid.* **216**, 713 (1977).
11. P. M. Solomon, G. R. Huguenin, N. Z. Scoville, *ibid.*, in press.
12. T. W. Hartquist, M. Oppenheimer, A. Dalgarno, *ibid.* **236**, 182 (1980).
13. H. R. Fetterman *et al.*, *Appl. Phys. Lett.* **33**, 151 (1978).
14. D. R. Williams, W. Lum, S. Weinreb, *Microwave J.* **23**, 73 (1980).
15. G. A. Koepf, in *Proceedings, Heterodyne Systems and Technology Conference* (Williamsburg, Va., 1980), p. 449; ——, H. R. Fetterman, N. McAvoy, *Int. J. Infrared Millimeter Waves* **1**, 597 (1980).
16. M. J. Mumma, Th. Kostiuk, D. Buhl, *Opt. Eng.* **17**, 50 (1978).
17. I. G. Nolt, T. Z. Martin, C. W. Wood, W. M. Sinton, *J. Atmos. Sci.* **28**, 238 (1971).
18. J. Waters, in *Submillimeter Wavelength Astronomy from Space* (Report 740-3, Jet Propulsion Laboratory, Pasadena, Calif., 1978).
19. On the best day we could easily detect Venus as well as the sun.
20. P. F. Goldsmith, *Astrophys. J.* **176**, 577 (1972).
21. ——, N. R. Erickson, H. R. Fetterman, B. J. Clifton, D. D. Peck, P. E. Tannenwald, G. A. Koepf, D. Buhl, N. McAvoy, *Astrophys. J.*, in press.
22. We thank C. D. Parker of Lincoln Laboratory for important contributions to the detector performance. A. Tokunaga provided valuable assistance at the IRTF. We also express our appreciation for the enthusiastic help of the IRTF operators. This work was supported in part by NSF grants AST78-18728 and AST79-19821 by NASA and by the IRTF through their Visiting Astronomer Program. The IRTF is operated by the University of Hawaii under contract from NASA.

19 September 1980; revised 24 November 1980

Virus in a Parasitoid Wasp: Suppression of the Cellular Immune Response in the Parasitoid's Host

Abstract. *A virus that replicates in the ovary of a parasitoid wasp is injected into the parasitoid's host during oviposition. Successful development of the parasitoid egg within the host depends on the presence of the virus, which acts to suppress the host's immune response (encapsulation) toward the egg. This is an example of obligatory mutualism between a virus and a eukaryotic organism.*

An indigenous virus (*1, 2*) exists in the ovaries of all females of several species of parasitoid wasps belonging to the family Ichneumonidae (*1-6*). These viruses replicate in the nuclei of calyx cells, an epithelial tissue located between the ovarioles and oviducts of the parisitoid (*3, 7*). The virus buds from the calyx cells into the lumen of the oviduct. As part of a calyx fluid, it is injected together with an egg into the hemocoel of host caterpillars. Subsequently, viral nucleocapsids enter host cells (*1, 6, 8*), apparently by a membrane-fusion event, and are uncoated within the nucleoplasm.

Crude calyx fluid (*9*) from the parasitoid wasp, *Campoletis sonorensis* (Hymenoptera: Ichneumonidae), interferes with host cellular immune defense mechanisms by suppression of parasitoid egg encapsulation (*10*), and inhibits host growth (*11, 12*). However, prior to our

Table 1. Host caterpillars, *Heliothis virescens*, were dissected 5 days after treatment to recover eggs or larvae of the parasitoid wasp, *Campoletis sonorensis*.

Host treatment	Eggs + larvae recovered (No.)	Encapsulated eggs (%)	Larvae (%)
a) Parasitized (control)	20	0	100
b) Egg + saline	36	100	0
c) Egg + calyx fluid	30	20	80
d) Egg + calyx fluid supernatant	20	100	0
e) Egg + ultraviolet-irradiated calyx fluid	35	100	0
f) Egg + purified virus	30	27	73
g) Egg + ultraviolet-irradiated purified virus	21	100	0
h) Virus-fed host; egg + saline	20	100	0